Measurement 140 (2019) 1–13

Contents lists available at ScienceDirect

Measurement

journal homepage: www.elsevier.com/locate/measurement

Knock detection based on the optimized variational mode decomposition

Bi Fengrong [a], Li Xin [a,*], Liu Chunchao [b], Tian Congfeng [b], Ma Teng [a], Yang Xiao [a]

[a] State Key Laboratory of Engines, Tianjin University, Tianjin 300072, China
[b] Shantui Construction Machinery CO., LTD, Jining 272000, China

ARTICLE INFO

Article history:
Received 21 May 2017
Received in revised form 3 February 2019
Accepted 20 March 2019
Available online 27 March 2019

Keywords:
Engine
Fault diagnosis
Knock
Variational Mode Decomposition (VMD)
Adaptive decomposition

ABSTRACT

In order to extract slight characteristics and achieve exact control of engine knock to improve the overall performance of engine, the optimized Variational Mode Decomposition (VMD) algorithm is introduced to process the vibration signals of engine. Combined with recursive model and energy difference tracking method, the optimized VMD can decompose signals into several modes based on stop criterion instead of artificial values set in advance. Besides, the initial values of center frequencies are also optimized for stability and efficiency. An analog signal is firstly decomposed by this method, and result shows that the optimized VMD has ability to extract components accurately. Then this method is applied for the decomposition of tested engine vibration signals and compared with the Empirical Mode Decomposition (EMD) and traditional VMD, the results show that the optimized VMD can eliminate effect of noise and extract knock at different intensities more accurately and quickly.

1. Introduction

As one of main power sources, engine draws much attention on its power and economy because of global energy and environmental crises. The down-sizing of engine, represented by turbocharger technology and gasoline direct injection, is an effective way to increase combustion efficiency of gasoline. With the development of down-sizing, knock increases significantly. Knock is an abnormal combustion phenomenon, which is caused by one or more pockets of air/fuel mixture explode outside the envelope of normal combustion front [1]. It will reduce the performance and useful life of engine greatly. However, slight knock is helpful in improving the combustion in engine, so it's necessary to detect and control engine knock precisely [2,3]. Common methods for knock detection include detecting combustion noise [4,5], collecting cylinder pressure [6,7], extracting block vibration features [8] and so on. Among these methods, detecting combustion noise is greatly affected by external factors [9]; collecting cylinder pressure is expensive and flimsy [10]; extracting block vibration features is widely used because of its low-cost, reliability and convenience [11]. The principle of detecting knock by vibration is that: high frequency oscillation in cylinders will transfer to block. Researchers collect and analyze vibration signals from sensors placed on block and then knock feature will be extracted. For example, Zadink et al. [12] used vibration signals of engine block to analyze knock.

However, engine block vibration signals contain very complex information. Its non-stationary character leads to poor detection precision which causes difficulty in detecting slight knock. Researchers have developed different algorithms for vibration signal processing, including traditional time-frequency analysis, wavelet transforms, the Empirical Mode Decomposition (EMD) [11–15] and so on. Traditional time-frequency analysis method such as Short Time Fourier Transform (STFT) cannot keep high-resolution both in time domain and frequency domain. Wavelet transform is essentially not an adaptive time-frequency analysis method [16]. For adaptive analysis methods, the EMD has insurmountable limitations because of its recursive decomposition model. The limitations, such as mode mixing, end effect, over and under decomposition, still puzzle researchers [17,18]. Although the Ensemble Empirical Mode Decomposition (EEMD) can alleviate mode mixing, it's followed by other problems. For example, the white noise (can't be eliminated completely) will cover weak energy signal and the increasing of computing time, which hobble the real-time diagnosis [19,20]. These problems seriously affect the practical application of those algorithms.

A new adaptive decomposition algorithm, Variational Mode Decomposition (VMD), was proposed by Dragomiretskiy et al. [21]. It is a non-recursive variational mode decomposition model, which is a generalization of the classic Wiener filter into multiple,

* Corresponding author.
E-mail address: nvh_lixin@tju.edu.cn (X. Li).

https://doi.org/10.1016/j.measurement.2019.03.042
0263-2241/

adaptive bands. Compared with EMD, the VMD is much more robust to sampling and noise.

There are various control parameters in VMD. Especially, the number of modes, K, is important for detecting knock in uncertain vibration signals and has a significant impact on over or under decomposition, which will result in mode mixing and ignoring for low power components. Many researchers tried to solve this problem and got three main methods. The first method is selecting a K value by prior knowledge. For example, Zipeng Li et al. [22] selected the K value by the number of local peaks in frequency domain. Fuhao Li et al. [23] selected the K value by effective modes number of the same signal decomposed by EEMD. The second method is searching a best K value for a specific signal by some indexes and using this parameter in subsequent computations. For example, Zhang et al. [24] searched a K value by energy and correlation coefficient. The third method is decomposing a signals with VMD in different K values and selecting the best one as final results. For example, Liu et al. [25] took scaling exponent as index and Wan et al. [26] took the degree of frequency mixing as index to decompose a signal from a presupposed K value until results met requirement. The first one is subjective and can't decompose a signal automatically, the K value selected by the second method is not suitable for all signals, the third one's calculation efficiency is too low. There is no recognized method to select K value. Therefore, the VMD should be further optimized to get modes by criterion adaptively.

This paper is organized as follows: VMD algorithm is briefly introduced in Section 2. The analysis of original VMD, optimization of VMD and its feasibility confirmed by the decomposition results of an analog is shown in Section 3. The experiment is described in Section 4. The Analysis, comparison and discussion for application of optimized VMD in knock detection are shown in Section 5. Conclusions and outlook are in Section 6.

2. VMD algorithm

The goal of VMD algorithm is to decompose an input signal f into several modes u_k. The u_k is defined as an amplitude modulation signal with limited bandwidth, and it compacts around the center pulsation ω_k [21].

First, VMD algorithm obtains the analytic signal of each mode u_k by the Hilbert transform, the $\mathrm{Au_k(t)}$ is:

$$\mathrm{A}u_k(t) = u_k(t) + \frac{\mathrm{j}}{\pi}\int_{-\infty}^{+\infty}\frac{u_k(v)}{t-v}dv = \left[\delta(t) + \frac{\mathrm{j}}{\pi t}\right] * u_k(t) \tag{1}$$

where the δ is Dirac distribution, j is the imaginary unit and $\mathrm{j}^2 = -1$.

Next, an estimated center frequency, $\mathrm{e}^{-\mathrm{j}\omega_k t}$, is mixed into the analytic signal, so the spectrum of mode will be modulated to the baseband, the $\mathrm{Bu_k(t)}$ is:

$$\mathrm{B}u_k(t) = \mathrm{A}u_k(t)\mathrm{e}^{-\mathrm{j}\omega_k t} = \left[\delta(t) + \frac{\mathrm{j}}{\pi t}\right] * u_k(t)\mathrm{e}^{-\mathrm{j}\omega_k t} \tag{2}$$

where the ω_k is the center frequency.

The bandwidth of mode can be obtained by computing its squared L^2-norm, so the constrained variational problem is as shown:

$$\left\{\begin{array}{c}\min\limits_{\{u_k\},\{w_k\}}\left\{\sum_k \| \partial_t\left[\left(\delta(t)+\frac{\mathrm{j}}{\pi t}\right) * u_k(t)\right]e^{-j\omega_k t}\|_2^2\right\} \\ \text{s.t.} \sum_k u_k = f\end{array}\right. \tag{3}$$

where $\{u_k\} := \{\mathrm{u_1}, \cdots, \mathrm{u_K}\}$ and $\{\omega_k\} := \{\omega_1, \cdots, \omega_K\}$ is the shorthand notations for the set of all modes and their center frequencies. The $\sum_k := \sum_{k=1}^{k}$ is the summation over all modes.

In order to solve the constrained variational problem, a quadratic penalty term α and Lagrange multipliers,λ, are introduced. The quadratic penalty term is used to encourage reconstruction fidelity, typically in the presence of additive Gaussian noise. The Lagrange multipliers can enforce constraints strictly. The augmented Lagrange is as shown:

$$L(\{u_k\},\{\omega_k\},\lambda) := \alpha\sum_k \| \partial_t\left[\left(\delta(t)+\frac{\mathrm{j}}{\pi t}\right) * u_k(t)\right]e^{-\mathrm{j}\omega_k t}\|_2^2 + \| f(t) - \sum_k u_k(t)\|_2^2 + \left\langle \lambda(t), f(t) - \sum_k u_k(t)\right\rangle \tag{4}$$

The quadratic problem can be solved easily in the Fourier domain [17]:

$$\widehat{u}_k^{n+1}(\omega) = \frac{\widehat{f}(\omega) - \sum_{i\neq k}\widehat{u}_i(\omega) + \frac{\widehat{\lambda}(\omega)}{2}}{1 + 2\alpha(\omega-\omega_k)^2} \tag{5}$$

$$\omega_k^{n+1} = \frac{\int_0^\infty \omega\left|\widehat{u}_k(\omega)\right|^2 d\omega}{\int_0^\infty \left|\widehat{u}_k(\omega)\right|^2 d\omega} \tag{6}$$

The Lagrange multipliers, λ, is that:

$$\widehat{\lambda}^{n+1}(\omega) = \widehat{\lambda}^{n}(\omega) + \tau\left(\widehat{f}(\omega) - \sum_k \widehat{u}_k^{n+1}\right) \tag{7}$$

The n is the number of iterations.

According to those, the original minimization problem is found as the saddle point of augmented Lagrange. Based on that, the Alternate Direction Method of Multipliers (ADMM) is used to update u_k, ω_k, λ The VMD algorithm is given in detail as follows:

① Initialize $\{u_k^1\}$, $\{\omega_k^1\}$, $\widehat{\lambda}^1$, n to 0;
② $n = n + 1$, and execution loop;
③ Update u_k by the formula (5);
④ Update ω_k by the formula (6);
⑤ Update λ by the formula (7);
⑥ Repeat step ②–⑤ until the iteration stop condition is met:

$$\sum_k\left(\| u_k^{n+1} - u_k^n\|_2^2 / \| u_k^n\|_2^2\right) < \varepsilon \tag{8}$$

When the loop completes, the input signal will be decomposed into K modes. The general value of ε is 1×10^{-7}.

3. The optimized VMD algorithm

The number of modes in VMD should be set in advance, but there is no selection criterion for that, which will cause over or under segmentation in decomposition of real vibration signals. So the VMD algorithm is optimized in order to achieve modes automatically and get Intrinsic Mode Functions (IMFs) with physical meanings.

3.1. The analysis of VMD

3.1.1. The analysis for number of modes in VMD

As mentioned above, the number of modes, K, in VMD has a great effect on results. In order to analyze the influence of K value on VMD, we use an analog signal to explain. The equations of this analog signal are as follows:

$$\begin{cases} s_1 = 30 * \sin\left(\frac{1}{18}\mathrm{fs} * \pi t + \frac{100}{3}\pi\right) \\ s_2 = \begin{cases} 200 * \sin\left(\frac{2500}{9}\mathrm{fs} * \pi t + \frac{5\times10^5}{3}\pi\right) & \text{if } t \in [0.0020\mathrm{s}, 0.0026\mathrm{s}] \\ 150 * \sin\left(\frac{2500}{9}\mathrm{fs} * \pi t + \frac{5\times10^5}{3}\pi\right) & \text{if } t \in [0.0056\mathrm{s}, 0.0058\mathrm{s}] \\ 100 * \sin\left(\frac{2500}{9}\mathrm{fs} * \pi t + \frac{5\times10^5}{3}\pi\right) & \text{if } t \in [0.0088\mathrm{s}, 0.0091\mathrm{s}] \\ 0 & \text{else} \end{cases} \\ s_3 = \eta \\ s_4 = 50 * \sin\left(\frac{5}{9}\mathrm{fs} * \pi t + \frac{1000}{3}\pi\right) \\ s = s_1 + s_2 + s_3 + s_4 \end{cases} \tag{9}$$

where $t \in [0, 0.01\mathrm{s}]$, the *fs* is sampling frequency, *fs* = 51200 Hz in this paper to correspond to the experiment in later section. s_1 is a low frequency sine signal, s_2 is an impact signal, η(i.e. s_3) is noise. To simulate actual situation, the noise in this paper is not the white Gaussian noise but only some random numbers in [-20, 20]. s_4 is a high frequency sine signal, *s* is the analog signal, as shown in Fig. 1.

The components of analog signal are known with the first peak in frequency domain corresponding to s_1, the second peak with wide bandwidth to s_2 and the last peak to s_4. According to [21], the best *K* value is 3. So, we decompose this analog signal under *K* = 2, 3, 4 to simulate under decomposition, normal decomposition and over decomposition respectively. The results are shown as Figs. 2–4.

As shown in Figs. 2–4, when *K* = 2, the result emerges under decomposition because VMD method doesn't extract impact component successfully. When *K* = 3, all components are extracted and there is no illusive component in result. When *K* = 4, although all components are extracted but the fourth mode is an illusive component (the frequency of s_3 is wide. So, it's not the noise component). This is only slight over decomposition. In order to analyze heavy over decomposition, we decompose this analog signal in *K* = 5. The result is shown as Fig. 5.

As shown in Fig. 5, when *K* = 5, the result emerges heavy over decomposition. The result not only obtains an illusive component (the fifth mode) but also decompose the impact component into two modes (the second and third modes).

In engine knock and other faults detection, under decomposition implies losing feature and over decomposition implies mode mixing. Therefore, in order to decompose signals with VMD accurately, we must select a suitable *K* value.

3.1.2. The analysis for initial center frequency in iteration

In original VMD, the core solving process is the iteration by ADMM, in which center frequency, ω_k, is the most easy to control. Dragomiretskiy et al. [21] provided three methods to control the iteration of center frequency: initializing ω_k to zero, initializing ω_k linearly and initializing ω_k randomly. Among those, initializing ω_k to zero is suitable for signals with narrow bandwidth in low frequencies; initializing ω_k linearly is suitable for signals with wide bandwidth, which have the same characteristic as engine vibration signals; initializing ω_k randomly leads to highly random results and can't be used in actual calculation. ω_k has a great effect on calculation efficiency and accuracy. If the initial values of ω_k is set properly, the iteration will converge quickly. This characteristic is very important for the algorithm proposed later. The two initialization methods are shown in Figs. 6 and 7. The *K* value is selected as 3 based on what mentioned above. (The input is still the signal shown in Fig. 1.)

As shown in Figs. 6 and 7, the iteration has a great effect on solving process. With zero initialization, the difference between initial center frequency values and the frequency characters of analog signal is so great that results in low accuracy (the frequency results are different from analog signal's) and low calculation efficiency (the iteration number of linear initialization is 29, the iteration number of zero initialization is 183). As mentioned above, we initialize the center frequencies as center frequencies of s_2, s_2, s_2, respectively. The result is shown as Fig. 8.

As shown in Fig. 8, the customized initialization has high accuracy and calculation efficiency (the iteration number is only 13). So in the algorithm proposed in this paper later, we will choose this customized initialization and the specific method will be described below.

3.2. Optimization method-A recursive VMD

As a variational model, VMD is much more accurate than recursive decomposition model, such as EMD. However, the recursive decomposition model has its unique advantage, i.e. it can decompose signals automatically by stop criterion instead of a predetermined decomposition level. The kernel idea of recursive decomposition model, taking EMD as an example, is that the input signal reduces the average of upper and lower

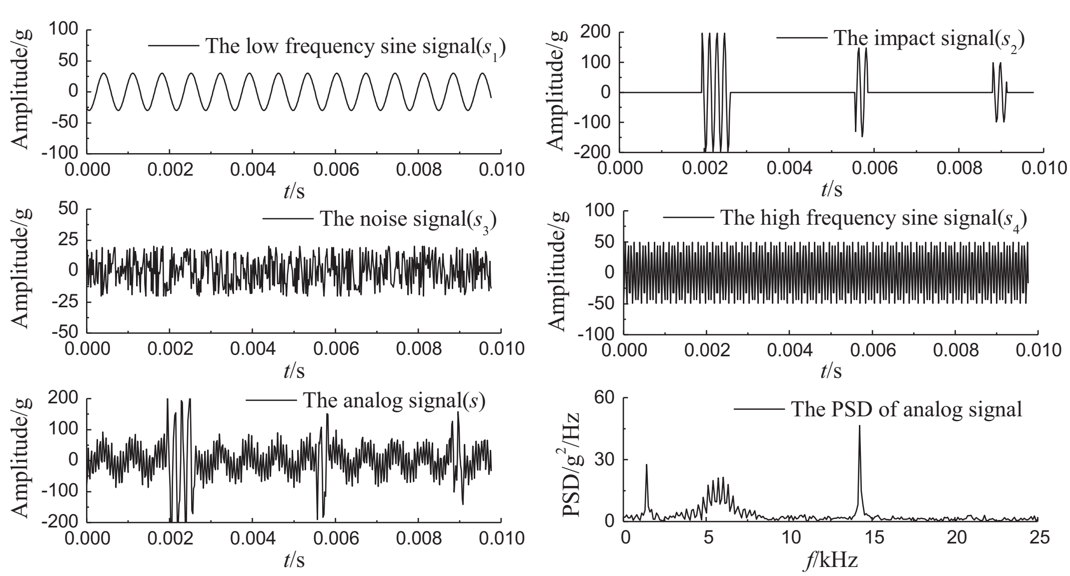

Fig. 1. The analog Signal.

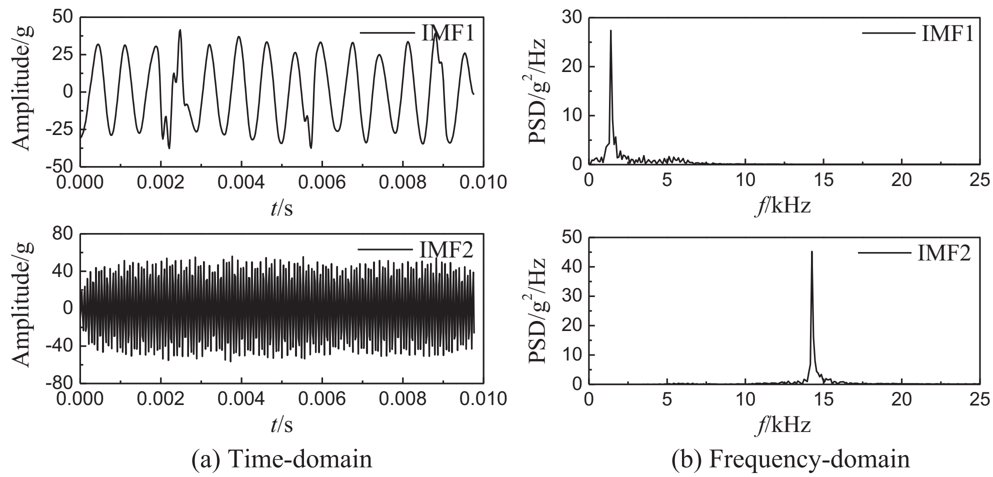

Fig. 2. The result of $K = 2$.

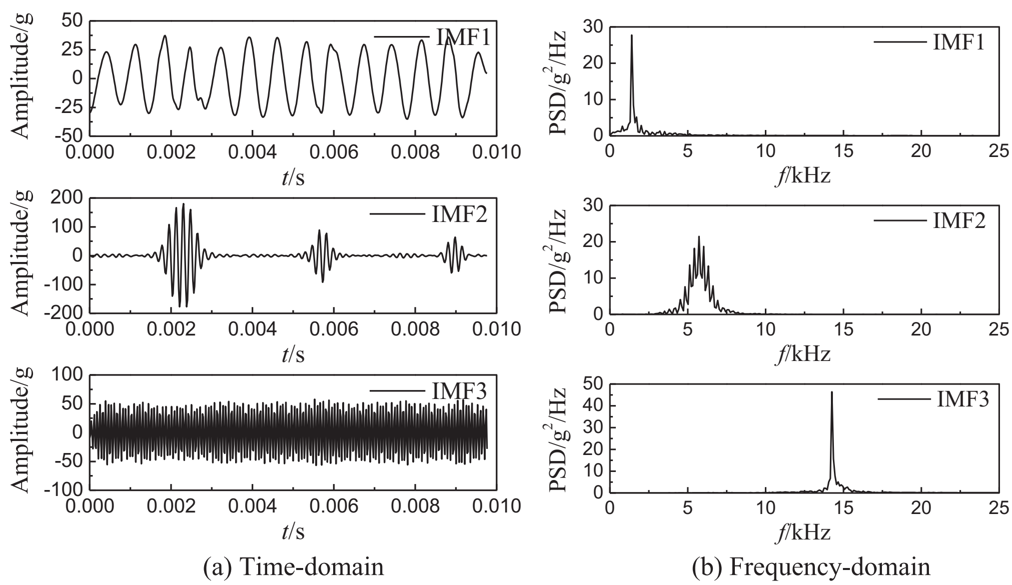

Fig. 3. The result of $K = 3$.

envelope curves until a requested IMF is obtained, and this process will repeat in order to decompose signal completely [16]. This process is described as "peeling onions". The upper and lower envelope curves are usually obtained by spline interpolation, which will gather errors in decomposition and result in mode mixing. Based on this analysis, we propose a recursive VMD algorithm, which combines variational model and recursive model. In this algorithm, IMFs are obtained by the variational model instead of envelope curves and then the decomposition is stopped by an appropriate criterion. With this method, the optimized algorithm will combine the advantages of recursive model and variational model to obtain desired results. This model can not only restrain error accumulation of envelopes in recursive model but also decompose signals automatically. The details of the algorithm are described below.

3.2.1. Adjustment of the variational model

Based on the original VMD [21], a new constrained variational problem can be achieved by setting the number of modes as $K = 1$. There is only one component u, and the Formula (3) changes into Formula (10):

$$\begin{cases} \min\limits_{u,\omega}\left\{\left\| \partial_t\left[\left(\delta(t)+\frac{j}{\pi t}\right)*u(t)\right]e^{-j\omega t}\right\|_2^2\right\} \\ \text{s.t}\, u = f \end{cases} \tag{10}$$

With the Lagrangian multipliers and quadratic penalty term, the augmented Lagrangian in Formula (4) changes into Formula (11):

$$L(u,\omega,\lambda) := \alpha\left\|\partial_t\left[\left(\delta(t)+\frac{j}{\pi t}\right)*u(t)\right]e^{-j\omega t}\right\|_2^2 + \| f(t)-u(t)\|_2^2 + \langle\lambda(t), f(t)-u(t)\rangle \tag{11}$$

The quadratic problem can be solved in Fourier domain, i.e. the Formula (5) and (6) change into Formula (12) and (13):

$$\hat{u}^{n+1}(\omega) = \frac{\hat{f}(\omega) - \frac{\hat{\lambda}(\omega)}{2}}{1+2\alpha(\omega_0-\omega)^2} \tag{12}$$

$$\omega^{n+1} = \frac{\int_0^\infty \omega\left|\hat{u}(\omega)\right|^2 d\omega}{\int_0^\infty \left|\hat{u}(\omega)\right|^2 d\omega} \tag{13}$$

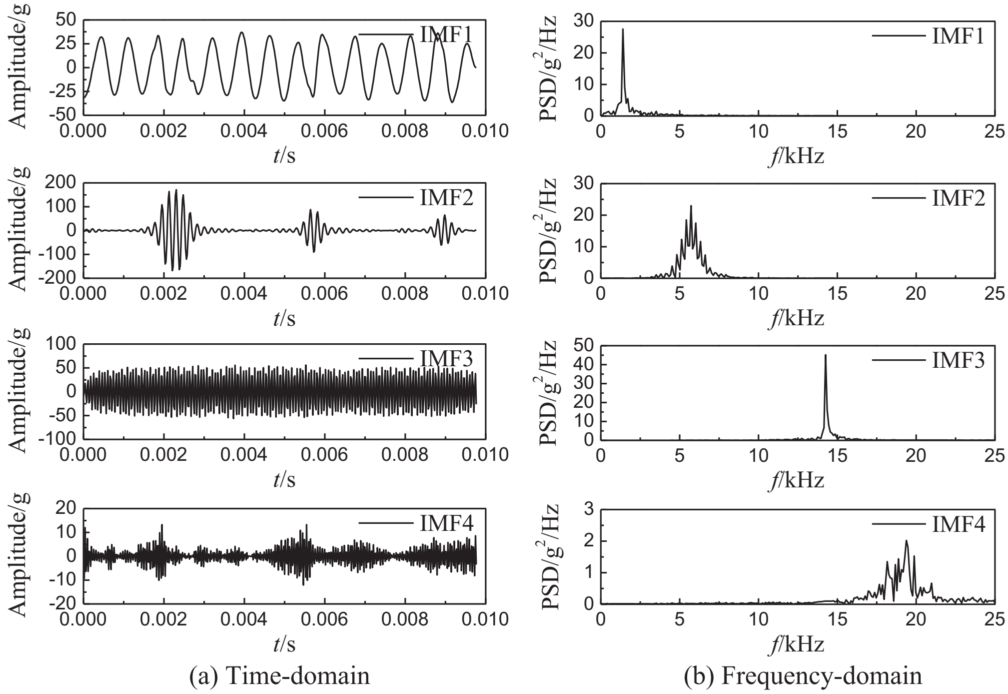

Fig. 4. The result of $K = 4$.

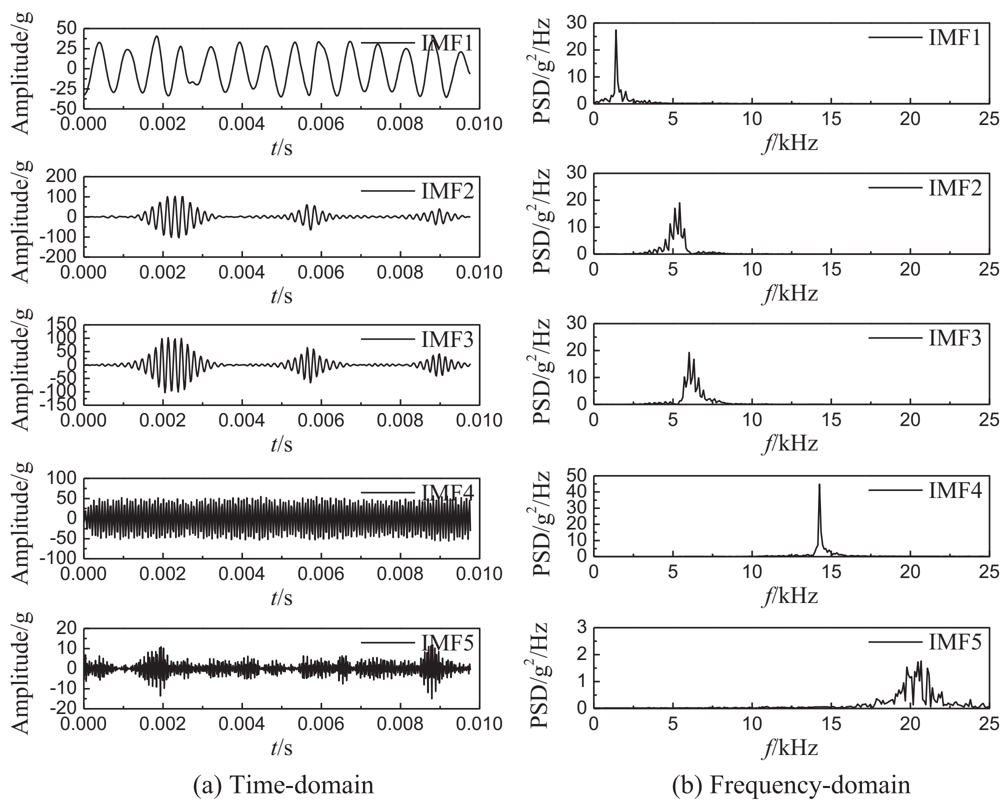

Fig. 5. The result of K = 5.

Except for this adjustment, the theory is the same as original algorithm, and it also can be explained as a special case, in which the number of modes is $K = 1$. After that, the VMD is taken as a single Wiener filter to process input signals in order to obtain the only one component u, and it will be the most significant feature of input signal without any adjustment. This process will extract components one by one in our model, which resembles the 'peeling onions' process of envelopes constructing in recursive model.

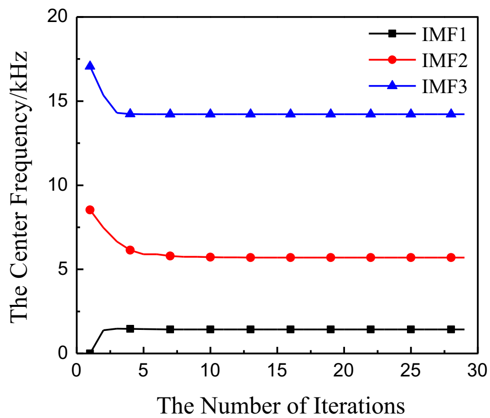

Fig. 6. The iterations of linear initialization.

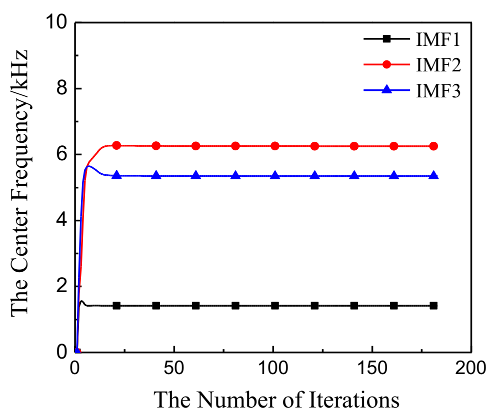

Fig. 7. The iterations of zero initialization.

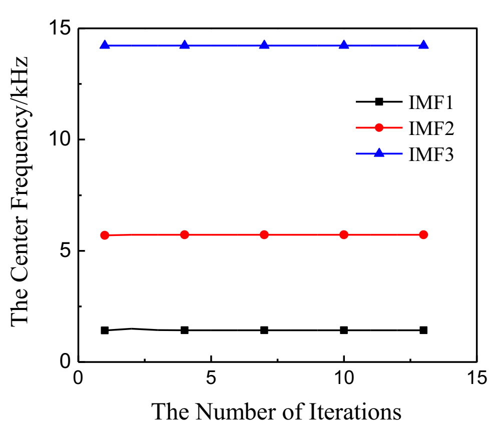

Fig. 8. The iterations of customized initialization.

3.2.2. Optimization of the initial values of center frequencies ω_k

When computing the center frequencies ω_k by ADMM in original VMD, the initial values must be input in advance. As mentioned above, Dragomiretskiy et al. [21] provided three types to select initial values: initializing the ω_k as 0, liner values and random values. Among those types, the liner values method has the highest computational efficiency and stability because it is more similar with most frequency characters, which is very useful for the ADMM iterative process. When $K = 1$, there is no liner values for initial values of ω_k, which causes the results to become unstable (just like initializing the ω_k as 0). As shown in Section 3.1.2, if the iterative initial values for center frequencies are set close to the characteristic frequencies of target components, accuracy and calculation efficiency will be improved greatly. Because the signal components are unknown, we choose to extract the component with the highest power in frequency domain firstly. Therefore, in order to obtain initial values, Power Spectral Density (PSD) of the input signal is calculated and the frequency at maximum PSD is taken as the initial value.

In particularly, because of the Gibbs phenomenon [27], sometimes the maximum PSD values are the endpoints. For this problem, the first 0.5% and the last 0.5% points in frequency domain will be ignored when processing real signals.

3.2.3. Stop criterion

To decompose signals automatically, the stop criterion must be chosen reasonably. Huang et al. [16] proposed a SD stop criterion, and Damerval et al. [28] proposed a stop criterion based on the number of iterations. Those stop criterions are proposed for recursive model and aren't suitable for VMD. However, the energy difference tracking method proposed by Cheng et al. [29] is built based on energy and this stop criterion is suitable for the method proposed in this paper. The basic assumption of this stop criterion is that the IMFs have orthogonality property. With comprehensive consideration of energy difference tracking method and the method proposed in this paper, the stop criterion is shown as follows:

Assuming that the signal $f(t)$ is made up of independent components $u_k(t)$:

$$f(\mathrm{t}) = u_1(t) + u_2(t) + \cdots + u_\mathrm{n}(t) = \sum_{k=1}^{\mathrm{n}} u_\mathrm{k}(t) \tag{14}$$

The total energy of $f(\mathrm{t})$ is:

$$E_\mathrm{x} = \int_{-\infty}^{\infty} f^2(t)dt = \int_{-\infty}^{\infty} \left[\sum_{k=1}^{n} u_k(t)\right]^2 dt \tag{15}$$

The independent components have orthogonality property, the formula (15) can be represented as:

$$E_\mathrm{x} = \int_{-\infty}^{\infty} \left[\sum_{k=1}^{n} u_k(t)\right]^2 dt = \int_{-\infty}^{\infty} u_1(t)dt + \int_{-\infty}^{\infty} u_2(t)dt + \ldots + \int_{-\infty}^{\infty} u_\mathrm{n}(t)dt$$
$$= E_1 + E_2 + \cdots E_n \tag{16}$$

When a component $u_1(t)$ is decomposed out, the total energy E_{tot} composed of the energy of $u_1(t)$, i.e. E_1 and the energy of the rest, i.e. $E_{2\cdots\mathrm{n}}$, is equal to the energy of original signal, i.e. E_x:

$$E_{tot} = E_1 + E_{2\cdots\mathrm{n}} = \mathrm{E}_x \tag{17}$$

If the independent components $u_k(t)$ are incomplete orthogonal, there will be error between E_x and E_{tot}:

$$\mathrm{E}_{err} = \mathrm{E}_x - E_{tot} = \mathrm{E}_\mathrm{x} - (E_1 + E_{2\cdots\mathrm{n}}) \tag{18}$$

The smaller $|\mathrm{E}_{err}|$ is, the orthogonality properties of IMFs better are, the rest of signal meets the requirements of IMF better. So the $|\mathrm{E}_{err}|$ is taken as the criterion and when the $|\mathrm{E}_{err}|$ is less than threshold, the decomposition will stop.

3.2.4. The proposed method

Based on above procedures, the optimized VMD is given. The flowchart of this algorithm is as shown in Fig. 9.

The specific process is as follows:

① Calculate the PSD of the input signal f and achieve the frequency at maximum PSD, ω_{ini};
② Take the ω_{ini} as initial value of center frequency in iteration, and set $K = 1$ to get the variational model as formula (11). Compute u_k and ω_k as formula (12) and formula (13) separately.

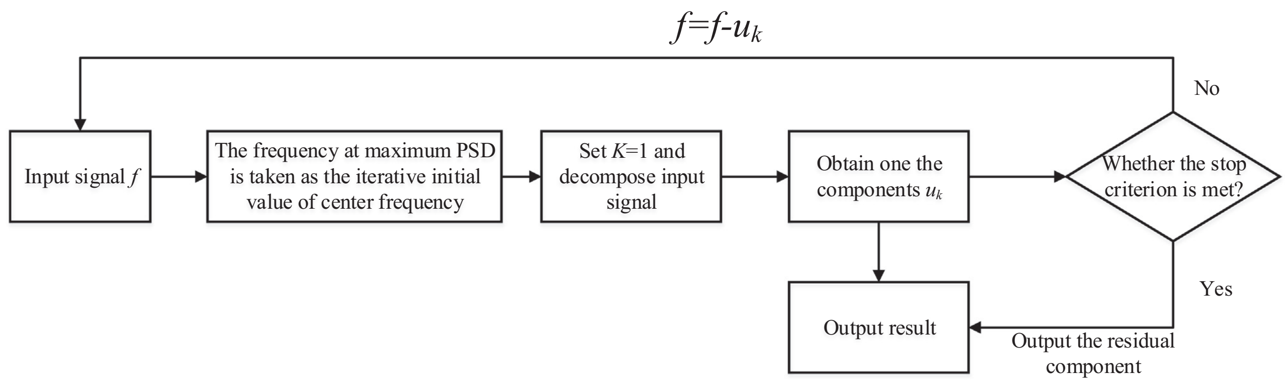

Fig. 9. The flowchart of the optimized VMD.

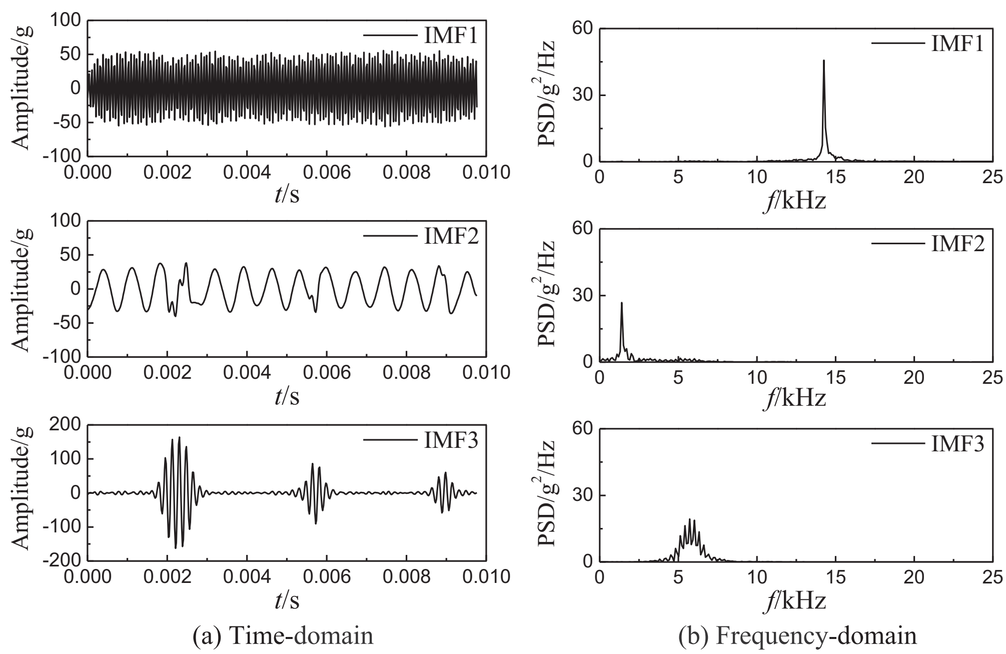

Fig. 10. The result of optimized VMD.

Table 1
The correlation coefficients between the result and original components.

The original components	s_1	s_2	s_4
The corresponding correlation coefficients	0.9904	0.9394	0.9315

③ Take the only one u_k as an IMF. Take the f - u_k as the new input signal and repeat step ① and ②;
④ At the same time of decomposition, the energy difference $|E_{err}|$ as formula (18) is calculated. When the $|E_{err}|$ is less than the threshold, the decomposition will stop and the component signals will be obtained automatically. Through calculation and experiment, $|E_{err}| \leqslant (0.7-2.0)\%\ E_x$ is considered as the appropriate threshold.

3.3. Confirmation of the optimized VMD algorithm

To confirm the feasibility of this optimized VMD, we adopt this method to decompose the analog signal shown in Fig. 1. Considering the noise, the stop criterion is set as $|E_{err}| \leqslant 1.5\%\ E_x$.

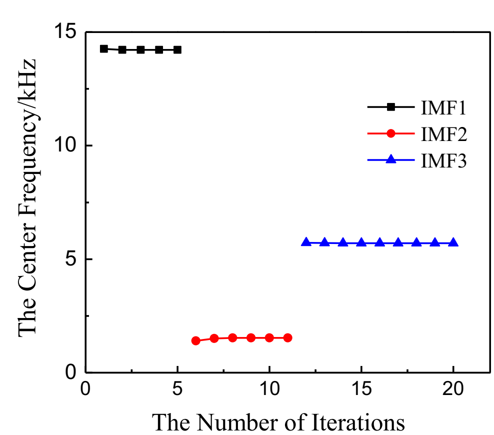

Fig. 11. The iteration process of optimized VMD.

When the analog signal was decomposed by original VMD, the number of modes is set as $K = 3$, which confirmed the best result. The optimized VMD decomposes the signal without setting up K, and the results are as shown in Fig. 10.

Table 2
The main parameters of test engine.

Items	Parameters
Combustion mode	Spark ignition
Arrangement	Inline
Number of cylinders	Four
Intake method	Turbocharger
Fuel injection method	Direct-injection
Displacement	1.5 L
Stroke/Bore	84.7/75 mm
Power rating	110 kW/5600 r/min
Torque rating	210 Nm/2200-4500 r/min

Table 3
The main test instruments and parameters.

The instruments	Model	Manufacturer
Acoustic and vibration testing system	SCM05	LMS
acceleration sensor	621B40	IMI SENSORS
Laptop	ThinkPad T530	Lenovo
Cylinder pressure sensor	GH13Z-31(24)	AVL

The results (without residual component) show that the optimized VMD can decompose the signal into correct decomposition level, $K = 3$, by the stop criterion, which confirms the feasibility of this optimized VMD proposed in this paper. The result also meets expected sequence in frequency domain. To validate the accuracy of optimized VMD quantifiably, we calculate the correlation coefficients between the result and original components shown in Fig. 1. The correlation coefficients are shown in Table. 1.

As shown in Table. 1, the accuracy of optimized VMD is still high. Besides, the optimized VMD has higher computational efficiency than original VMD. The number of iterations in original VMD with linear initialization is 29 as shown in Fig. 6. The number of iterations in optimized VMD is 20 and the three numbers are 5, 6, 9, separately, as shown in Fig. 11.

As shown in Fig. 11, the number of iterations in optimized VMD is fewer, which means higher calculation efficiency. It also can obtain more stable results with no mode mixing. Therefore, the proposed method is meaningful to overcome the shortage of the VMD and take the algorithm to decompose real signal with unknown number of sources.

4. The experiment

The knock experiment is carried out on a turbo charged gasoline direct-injection engine, and the basic information of this engine is shown in Table 2. Two acceleration sensors are installed on the cylinder head above the second and third cylinders separately. A speed sensor is installed on flywheel to collect speed signals and identity the top dead center. Four cylinder pressure sensors are installed in all of the cylinders to collect cylinder pressure signals, and those signals will be passed to combustion analyzer and acoustic & vibration testing system separately. The main instruments of this signal testing system are shown in Table 3. Considering that the characteristic frequency of knock is about 5–20 kHz, the sampling frequency is set as 51.2 kHz. Microphones are put next to testing engine and connected to a speaker to detect knock sound. The experimental testing is shown as Fig. 12.

The range of engine speed is from 1200 r/min to 5600 r/min every 400 r/min and the range of engine torque is from 70 N•m to 205 N•m every 5 N•m. Because of the high frequency of knock in the speed range of 1400 r/min to 1600 r/min for testing engine, the 1400 r/min and 1500 r/min working conditions are added. The sound form speaker and the output form combustion analyzer will be used to judge the knock and its intensity preliminarily. During testing, knock will be controlled by spark advance angle and the spark advance angle increases by 2° Crank Angle (CA) form normal condition to knock appearance. However, if there is no knock until torque decreases obviously, this working condition will be recognized as no-knock condition.

Fig. 12. The bench test.

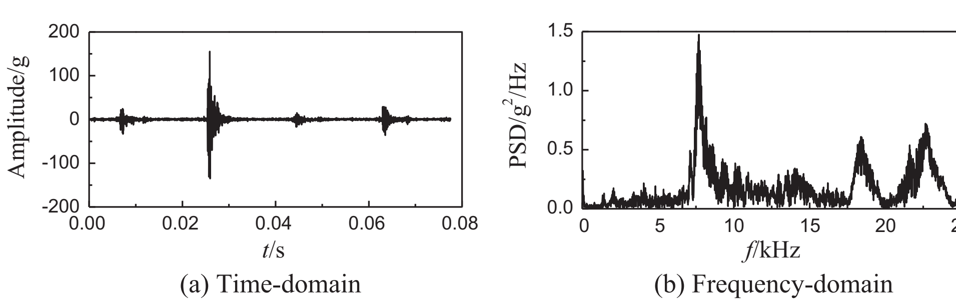

Fig. 13. A vibration signal.

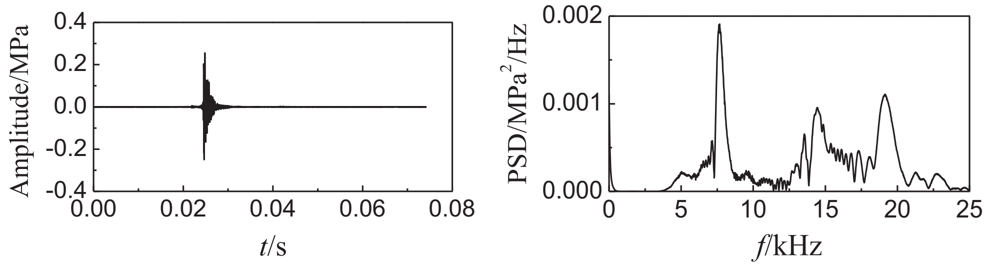

(a) Time-domain (b) Frequency-domain

Fig. 14. The pressure signal of the second cylinder.

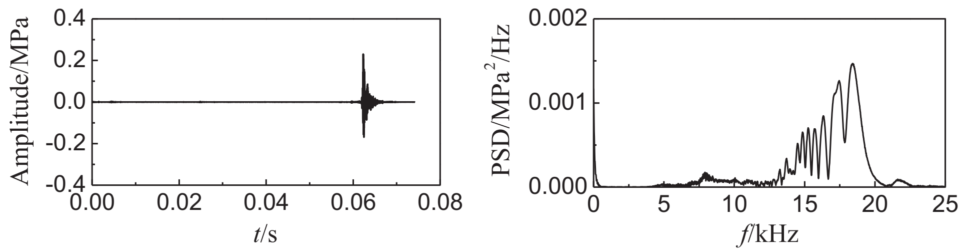

(a) Time-domain (b) Frequency-domain

Fig. 15. The pressure signal of the third cylinder.

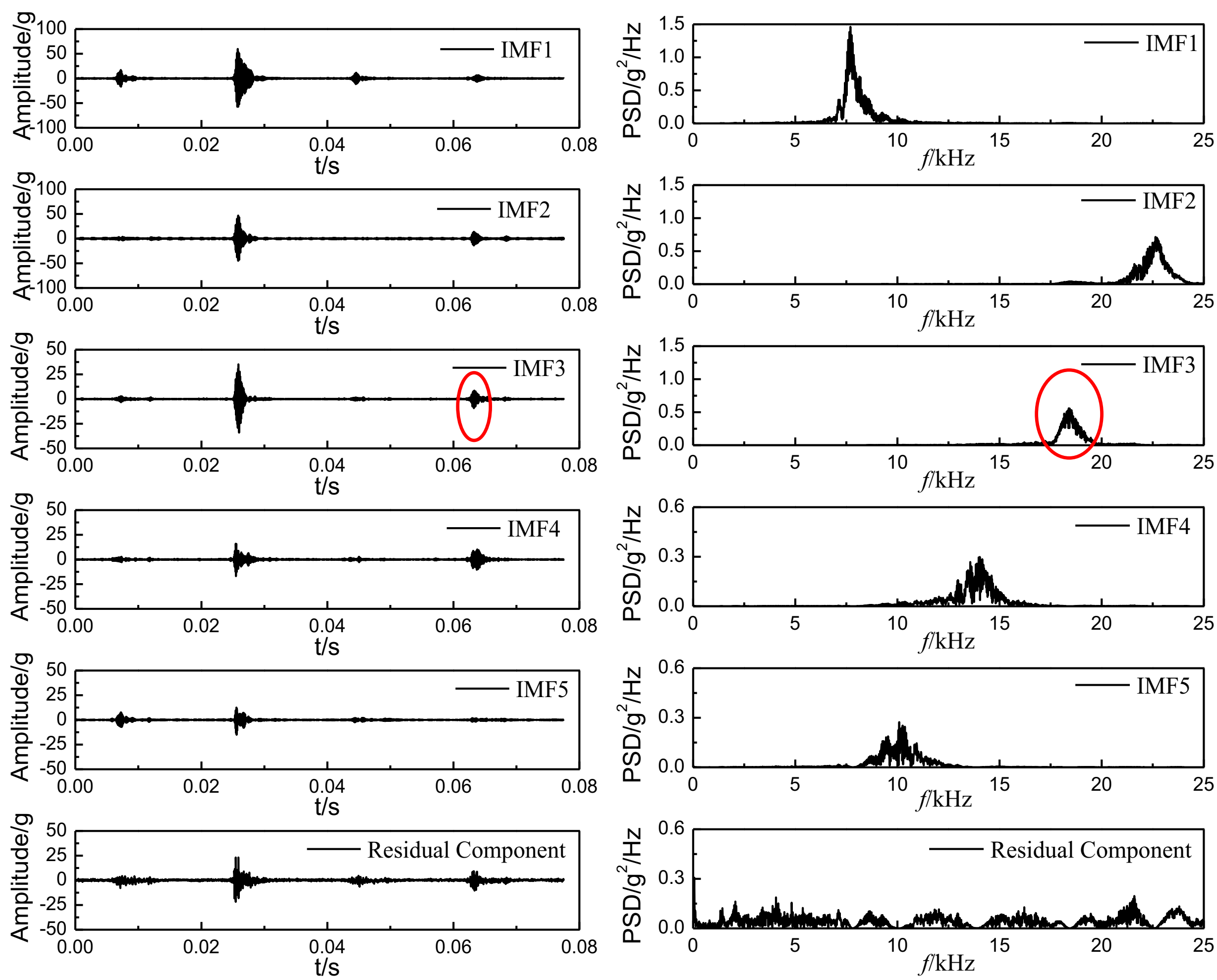

(a) Time-domain (b) Frequency-domain

Fig. 16. The result of optimized VMD.

5. Analysis, comparison and discussion

In this section, the optimized VMD is used to decomposed engine vibration signals in order to extract knock features.

5.1. The preliminary analysis of signals

The vibration signals of engine block under normal and knock conditions are collected. A randomly selected knock signal and its PSD are shown in Fig. 13. In this signal, the firing sequence is 4-2-1-3. The engine working condition is like this: the speed is 1600 r/min and the ignition advance is pushed forward 10° CA compared with normal condition. The vibration signal originates in the vibration sensor installed on the third cylinder head.

In consideration of that the main high-frequency vibration of block is excited by the combustion pressure fluctuations in cylinders, the cylinder pressure signals corresponding to vibration signals are also analyzed (it's verification for later decomposition results, too). The pressure signals are approached by 5 kHz high-pass filtering. The knock cylinders are the second cylinder and the third cylinder, and the time-domain and frequency-domain of pressure signals are shown in Figs. 14 and 15.

As shown in Figs. 14 and 15, the frequency band of knock is composed of some discrete frequencies between 5 kHz and 20 kHz and there is no frequency higher than 20 kHz in the cylinder pressure signals. Based on the analysis of the engine, the frequency components higher than 20 kHz in vibration signals are confirmed to come from turbocharger. Besides, the strong knock in the second cylinder can be detected by vibration signals, but the slight knock in the third cylinder can't (that is the components caused by the third cylinder will be covered by second cylinder's). So the vibration signals should be decomposed by VMD.

5.2. Comparison of optimized VMD and EMD

The vibration signal shown in Fig. 13 is decomposed by optimized VMD and EMD respectively. The results of optimized VMD have 6 modes including residual component, and the results of EMD has 12 modes. In this paper, all modes of optimized VMD and the first 6 modes of EMD are shown in Figs. 16 and 17.

As shown in Figs. 16 and 17, without filtering, the results of optimized VMD are valuable narrow-band modes. Besides, the center frequencies of first 5 modes in optimized VMD are 7.7 kHz, 22.6 kHz, 18.4 kHz, 14.0 kHz, 10.1 kHz, and the residual component is complex noise. The results can distinguish vibration caused by normal combustion, slight knock (red circle marker in Fig. 16, i.e. IMF3), strong knock and turbocharger clearly. In particular, the IMF3 of optimized VMD is only caused by the third cylinder pressure which means the slight knock in the third cylinder can be extracted obviously. The order of component frequencies also verifies the stability provide by customized initialization (the energy of every component in frequency domain is from high to

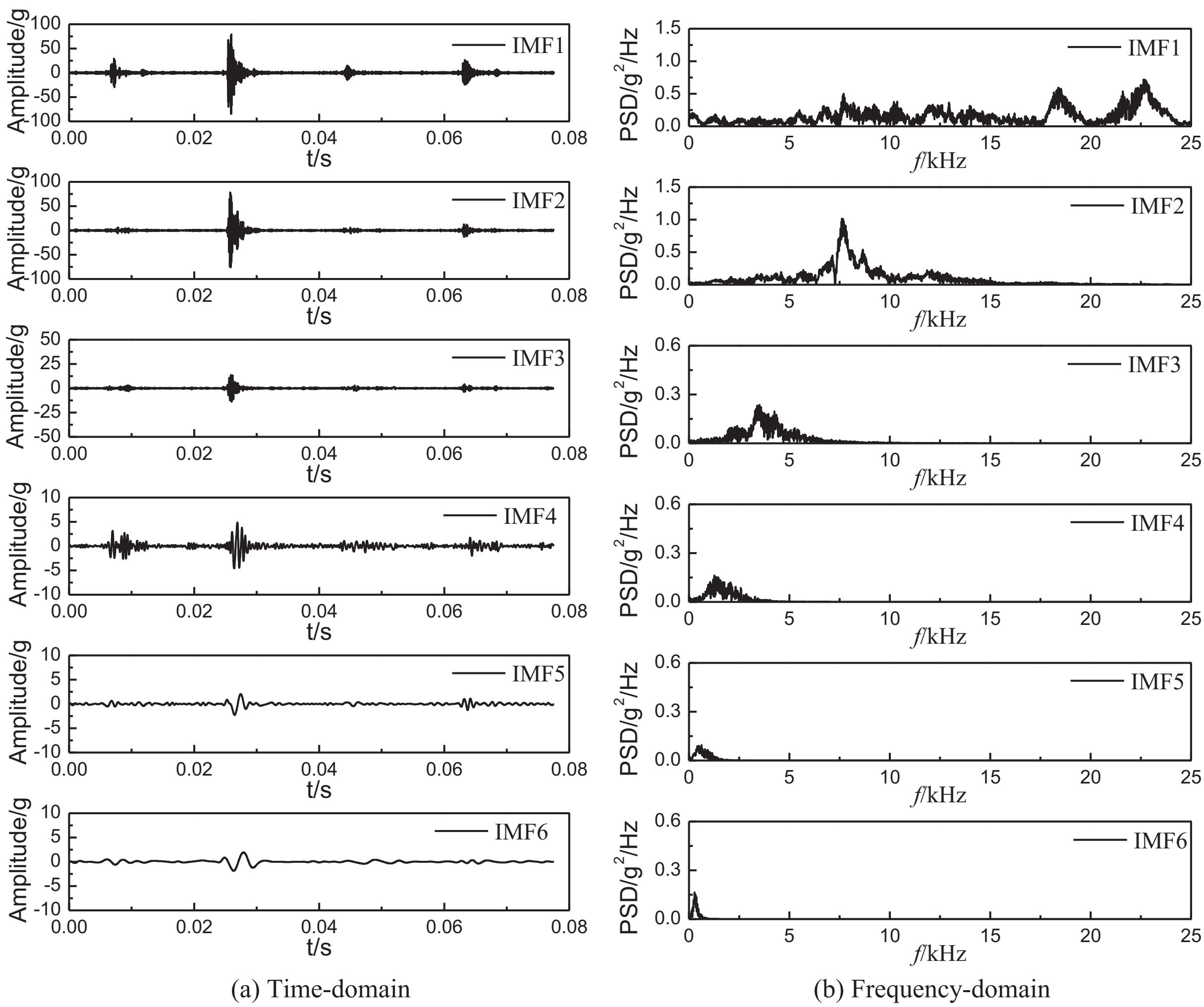

Fig. 17. The result of EMD.

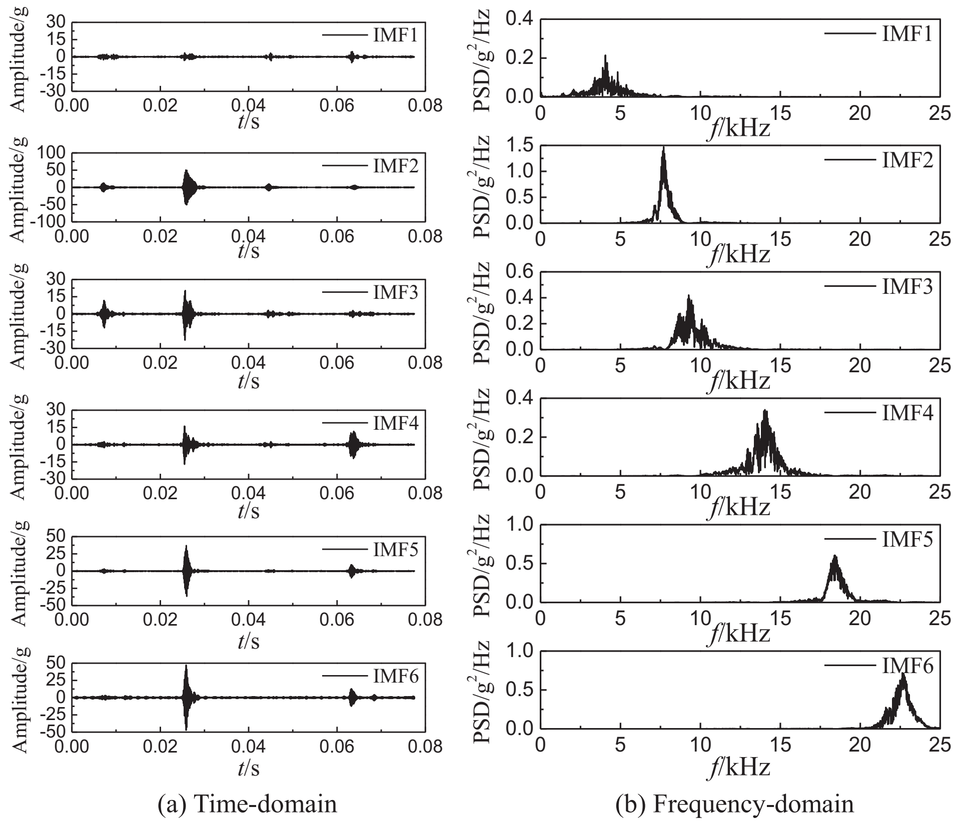

Fig. 18. The result of VMD based on search method.

low). Compared with VMD, EMD can also detect the strong knock in the second cylinder, but the slight knock in the third cylinder cannot be extracted. Besides, the disturbing factor from turbocharger can't be removed. The reason is that the frequencies of modes from VMD algorithm focused on knock characteristic frequencies, which means there is less noise in modes. As to EMD, the frequency components are complex, and there is much noise in modes. For knock detection, it is essential to remove noise form modes and make the knock feature obvious. To make the results credible, we give a quantized explain as follows. Because the frequency band of knock is composed of some discrete frequencies between 5 kHz and 20 kHz, we extract the knock components of original signal (shown in Fig. 13) by band-pass filtering form 5 kHz to 20 kHz. Based on the attention to energy in knock detection, the knock components of optimized VMD (i.e. IMF1/IMF3/IMF4/IMF5) and EMD (i.e. IMF1/IMF2) are restructured separately and their energy will be calculated to be compared with filtered original signal. The results show that the energy in optimized VMD restructure component is 81.22% of filtered original signal, and this value for EMD is 141.25%. Considering the noise exist in filtered original signal, the result of optimized VMD is reasonable and advantageous to slight knock detection. However, the result of EMD shows that there is much noise in it. This noise is mainly from turbocharger and will cover up slight knock features. In conclusion, the optimized VMD is much more advantageous than EMD in knock detection, even the accuracy is close to the detection method using cylinder pressure.

It should be noted that we don't use band-pass filtering to detect knock because the bands of knock character frequencies can't be detected exactly. That is to say, the noise in filtered signals is uncontrollable, which will result in difficulty for knock index and precise control.

5.3. Comparison of optimized VMD and VMD based on search method

In [26], the authors proposed a VMD method that decomposed a signal in different K values and the best K value will be selected by the degree of frequency mixing. Our team also use a similar method to decompose vibration signals to extract knock features [30], which is decomposing signals with VMD in a small K value and increasing it one by one until the center frequency differences between neighbouring components meet a predefined threshold. We set the threshold like this: the range of the maximum center frequency difference is 3.0–8.0 kHz and the minimum value is 1.0–2.5 kHz. With this method, we decompose the signal shown in Fig. 13 and there are 6 modes in this result as shown in Fig. 18.

This VMD based on search method decompose a signal with original VMD in different parameters. The original VMD has been proved the high accuracy [21], which means the VMD based on search method maintains high accuracy. In particular, we also calculate the energy of this results, and it is 81.15% of filtered original signal. This is very close to the value of optimized VMD proposed in this paper (81.22%, see the Section 5.2), which also proves the optimized VMD proposed in this paper maintains high accuracy of original VMD.

However, the VMD based on search method has low calculation efficiency. If we set the initial K value is 3, the iterations are shown in Fig. 19 and the iterations of optimized VMD in this paper are shown in Fig. 20.

The optimized VMD proposed in this paper has 5 iterations (the last component is residual), and the number of every iteration is 9, 11, 9, 20, 22 respectively with total number of 71. The VMD based search method has 4 iterations, the number of every iteration is 191, 243, 52, 190, and the total number is 676. Even when $K = 6$, the number is up to 190, which is far more than 71.

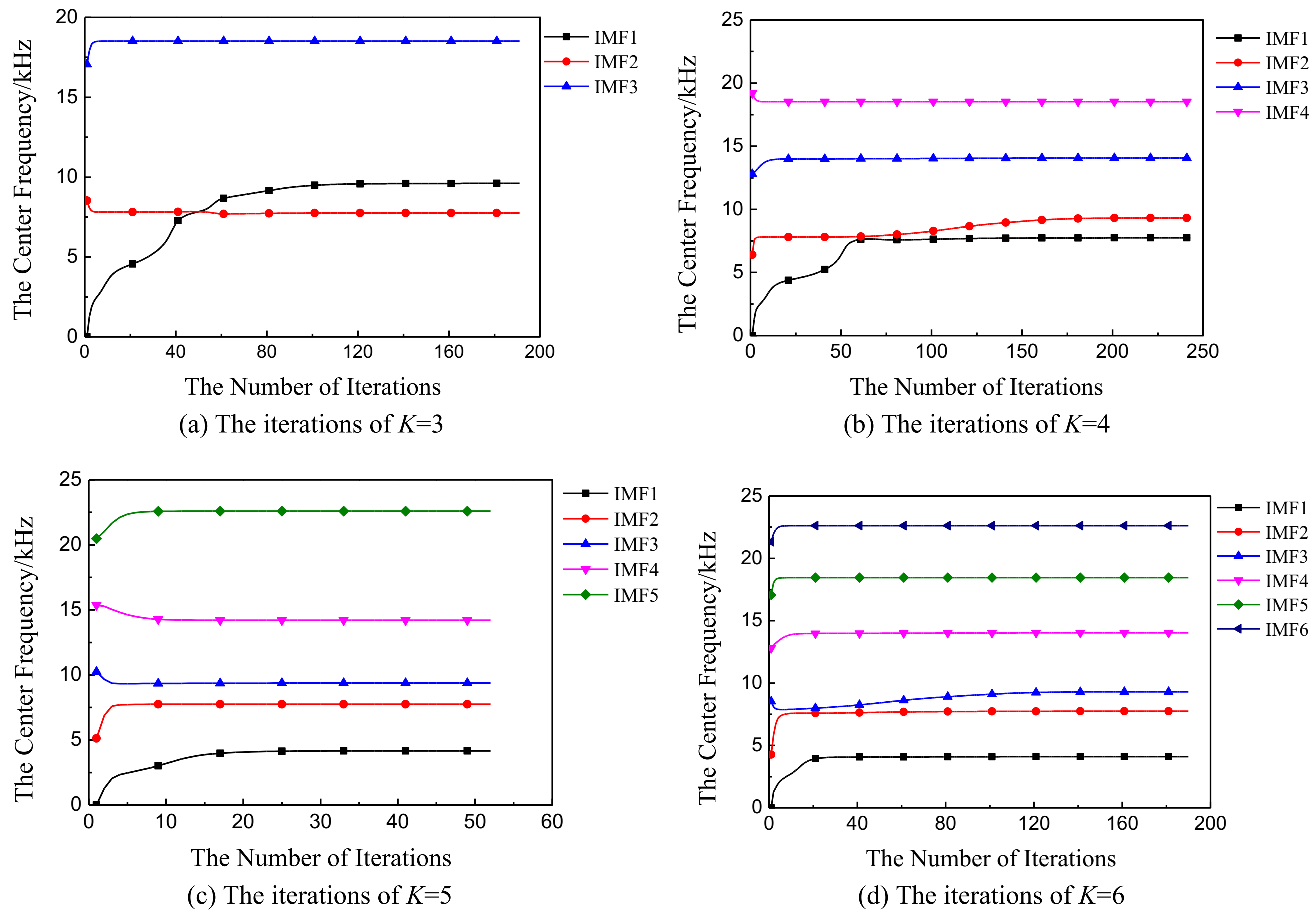

Fig. 19. The iterations of VMD based search method.

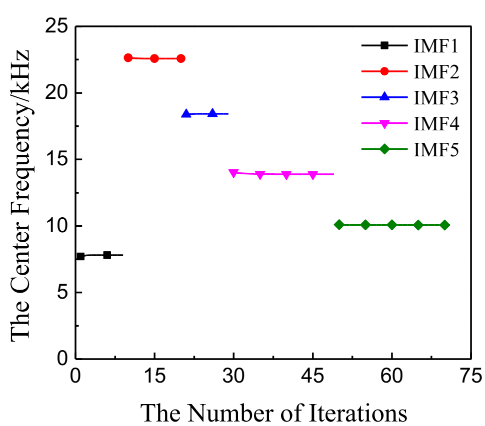

Fig. 20. The iterations of optimized VMD proposed in this paper.

In conclusion, the optimized VMD proposed in this paper has high calculation efficiency with high accuracy and this method is expected to be applied to detect knock and other engine faults.

5.4. Discussion

5.4.1. Error analysis

The main errors in detecting knock by vibration signals usually come from testing system and signals analysis algorithm.

The main error in testing system comes from acceleration sensors. The acceleration sensors used in this experiment has a range of 500 g, sensitivity of 0.02 m/s^2, and transverse sensitivity of $\leq 5\%$. As shown in these parameters, the error caused by acceleration sensors is acceptable.

The main error in VMD algorithm comes from the quadratic penalty term α and this parameter is related to bandwidth of modes in results. In [31], the authors adjusted α after decomposition every time. In consideration of difference of different signals and calculation efficiency, we set a fixed α value. According to the results from previous analysis, we set $\alpha = 2200$. However, this parameter is the best value for original VMD and has not yet been proved to be effective in this optimized VMD (although we get accuracy results with this value). Meanwhile, we find when α increases, the stop criterion will also increase. We think the reason for that is with increasing of α, the noise in components will decrease, which results in increasing energy difference. The quantized relationship between α and stop criterion is complex, and it is an important topic in our team. In this paper, these parameters are $\alpha = 2200$ and $|E_{err}| \leqslant 0.7\%\ E_x$separately.

5.4.2. Universal applicability analysis

To test the universal applicability of the optimized VMD, a large number of vibration signals are collected. In this paper, 100 signals in various working conditions are selected randomly to be decomposed by optimized VMD. All results get normal combustion, light knock and strong knock features successfully. The stop criterion is set as $|E_{err}| \leqslant 0.7\%\ E_x$, and there is no signal inappropriate for this method in our data. The results are not shown in this paper because of the limited space, and readers can test the universal applicability by your own data.

6. Conclusions and outlook

With the analysis of knock detection methods, the recursive decomposition model is deprecated and an entirely non-recursive variational decomposition model is introduced. However, the number of modes in VMD should be set in advance. So an optimized VMD algorithm combined recursive model, the energy difference tracking method and optimized initial values of center frequencies is proposed. The optimized VMD can decompose signals into modes based on stop criterion instead of artificial values set in advance.

In decomposition of analog and actual signals, the results show that the optimized VMD achieves expected effect. Compared with EMD and VMD based search method, the optimized VMD algorithm can reduce more noise and make the knock characteristics more obvious, which is helpful to detect slight knock to control engine precisely. All the decomposition results show that the optimized VMD has better accuracy, efficiency and stability.

However, the quantized relationship between α and stop criterion is still unclear. An appropriate knock intensity index for optimized VMD results should be developed, which will be our subsequent works.

Acknowledgments

The financial sponsorship of this work is from the National Science and Technology Support Program of China (2015BAF07B04). It is also sponsored by the Tianjin University State Key Laboratory of Engines.

Appendix A

The list of symbols

t	Time
f	Frequency
K	The Number of Modes
u	Component Signal
j	The Imaginary Unit, $j^2 = -1$
δ	Dirac Distribution
α	The Balancing Parameter of the Data-Fidelity Constraint (The Quadratic Penalty Term)
ω	The Center Frequency
λ	The Lagrangian Multiplier
ω_{ini}	The Initial Value of Center Frequency in Iteration

Appendix B

The list of abbreviations

EMD	Empirical Mode Decomposition
EEMD	Ensemble Empirical Mode Decomposition
STFT	Short Time Fourier Transform
VMD	Variational Mode Decomposition
ADMM	Alternate Direction Method of Multipliers
IMF	Intrinsic Mode Function
PSD	Power Spectral Density
CA	Crank Angle

References

[1] A.D. Eisner, D.E. Rosner, Experimental and theoretical studies of submicron particle thermophoresis in combustion gases, Pch Physicochem. Hydrodyn. 7 (2) (1986) 91–100.
[2] S. Patrik, B. Hannes, P. Philippe, et al., Micro-thermal CMOS-based gas quality sensing for control of spark ignition engines, Measurement 91 (2016) 661–679.
[3] Y. Nilsson, E. Frisk, L. Nielsen, Weak knock characterization and detection for knock control, Proc. Mech. Eng. 223 (1) (2009) 107–129.
[4] D. Siano, M.A. Panza, Sensitivity analysis of knock indices and combustion noise evaluation for S.I. engine, Int. Rev. Model. Simul. 7 (6) (2014) 1003–1101.
[5] F. Bozza, S. Fontanesi, A. Gimelli, et al., Numerical and experimental investigation of fuel effects on knock occurrence and combustion noise in a 2-stroke engine, SAE Int. J. Fuels Lubr. 5 (2) (2012) 674–695.
[6] G. Enzo, Dynamic knock detection and quantification in a spark ignition engine by means of a pressure based method, Energy Convers. Manage. 64 (2012) 256–262.
[7] W. Zhi, W. Yue, D.R. Rolf, Pressure oscillation and chemical kinetic coupling during knock processes in gasoline engine combustion, Energy Fuels 26 (2012) 7107–7119.
[8] Fengrong B, Teng M, Jian Z. Knock feature extraction in spark ignition engines using EEMD-Hilbert transform. SAE Technical Paper 2016-01-0087, 2016.
[9] K. Jafarian, M. Mobin, M.R. Jafari, et al., Misfire and valve clearance faults detection in the combustion engines based on a multi-sensor vibration signal monitoring, Measurement 128 (2018) 527–536.
[10] C. Guardiola, B. Pla, P. Bares, et al., Cylinder charge composition observation based on in-cylinder pressure measurement, Measurement 131 (2019) 559–568.
[11] Y. Wang, Research on knock diagnosis and control strategy of gasoline engine, Harbin Institute of Technology, Harbin, 2010.
[12] Zadnik M, Vincent F, Vingerhoeds R, et al. SI Engine Knock Detection Method Robust to Resonance Frequency Changes. SAE paper, 2007-24-0054, 2007.
[13] A. Ken, K. Hirotaka, K. Atsushi, Development of pattern recognition knock detection system using short-time Fourier transform, Advances in Automotive Control 46 (21) (2013) 366–371.
[14] D. Siano, D. Agostino, Knock detection in SI engines by using the discrete wavelet transform of the engine block vibrational signals, Energy Procedia 81 (2015) 673–688.
[15] T.A. Ahmad, G. Barat, T. Teymour, et al., Characterization of engine's combustion-vibration using diesel and biodiesel fuel blends by time-frequency methods: a case study, Renewable Energy 95 (2016) 422–432.
[16] N.E. Huang, Z. Shen, S.R. Long, et al., The empirical mode decomposition and the Hilbert spectrum for nonlinear and non-stationary time series analysis, Math. Phys. Eng. Sci. 454 (1971) (1998) 903–995.
[17] B. Chen, Z. He, X. Chen, et al., A demodulating approach based on local mean decomposition and its application in mechanical fault diagnosis, Meas. Sci. Technol. 22 (2) (2009) 28.
[18] S Zheng J, Cheng J, Yang Y. A rolling bearing diagnosis approach based on LCD and fuzzy entropy. Mech. Mach. Theory, 2013, 70: 441-453.
[19] J.R. Yeh, J.S. Shieh, N.E. Huang, Complementary ensemble empirical mode decomposition: a novel noise enhanced data analysis method, Adv. Adapt. Data Anal. 2 (2) (2010) 135–156.
[20] X. Xue, J. Zhou, Y. Xu, et al., An adaptively fast ensemble empirical mode decomposition method and its applications to rolling element bearing fault diagnosis, Mech. Syst. Sig. Process. 62 (2015) 444–459.
[21] K. Dragomiretskiy, D. Zosso, Variational mode decomposition, IEEE Trans. Signal Process. 62 (3) (2014) 531–544.
[22] L. Zipeng, C. Jinglong, Z. Yanyang, et al., Independence-oriented VMD to identify fault feature for wheel set bearing fault diagnosis of high speed locomotive, Mech. Syst. Sig. Process. 85 (2017) 512–529.
[23] L. Fuhao, L. Rong, T. Lili, et al., Data-driven time-frequency analysis method based on variational mode decomposition and its application to gear fault diagnosis in variable working conditions, Mech. Syst. Sig. Process. 116 (2019) 462–479.
[24] Z. Ming, J. Zhinong, F. Kun, Research on variational mode decomposition in rolling bearings fault diagnosis of the multistage centrifugal pump, Mech. Syst. Sig. Process. 93 (2017) 460–493.
[25] L. Yuanyuan, Y. Gongliu, L. Ming, et al., Variational mode decomposition denoising combined the detrended fluctuation analysis, Signal Process. 125 (349) (2016) 364.
[26] W. Shuting, Z. Xiong, D. Longjiang, Compound fault diagnosis of bearing using improved spectral kurtosis with VMD, J. Mech. Sci. Technol. 32 (11) (2018) 5189–5199.
[27] C.W. Onneweer, The Wilbraham-Gibbs phenomenon in Fourier analysis, Math Medley 2 (1982) 47–54.
[28] C. Damerval, S. Meignen, Valérie Perrier. A fast algorithm for bidimensional EMD, IEEE Signal. Process. Lett. 12 (10) (2005) 701–704.
[29] J. Cheng, D. Yu, Y. Yu, Research on the intrinsic mode function (IMF) criterion in EMD method, Mech. Syst. Sig. Process. 20 (4) (2006) 817–824.
[30] F. Bi, X. Li, T. Ma, Knock detection using variational mode decomposition, J. Vib. Meas. Diagn. 38 (5) (2018) 903–907.
[31] J. Xingxing, W. Jun, S. Juanjuan, et al., A coarse-to-fine decomposing strategy of VMD for extraction of weak repetitive transients in fault diagnosis of rotating machines, Mech. Syst. Sig. Process. 116 (2019) 668–692.